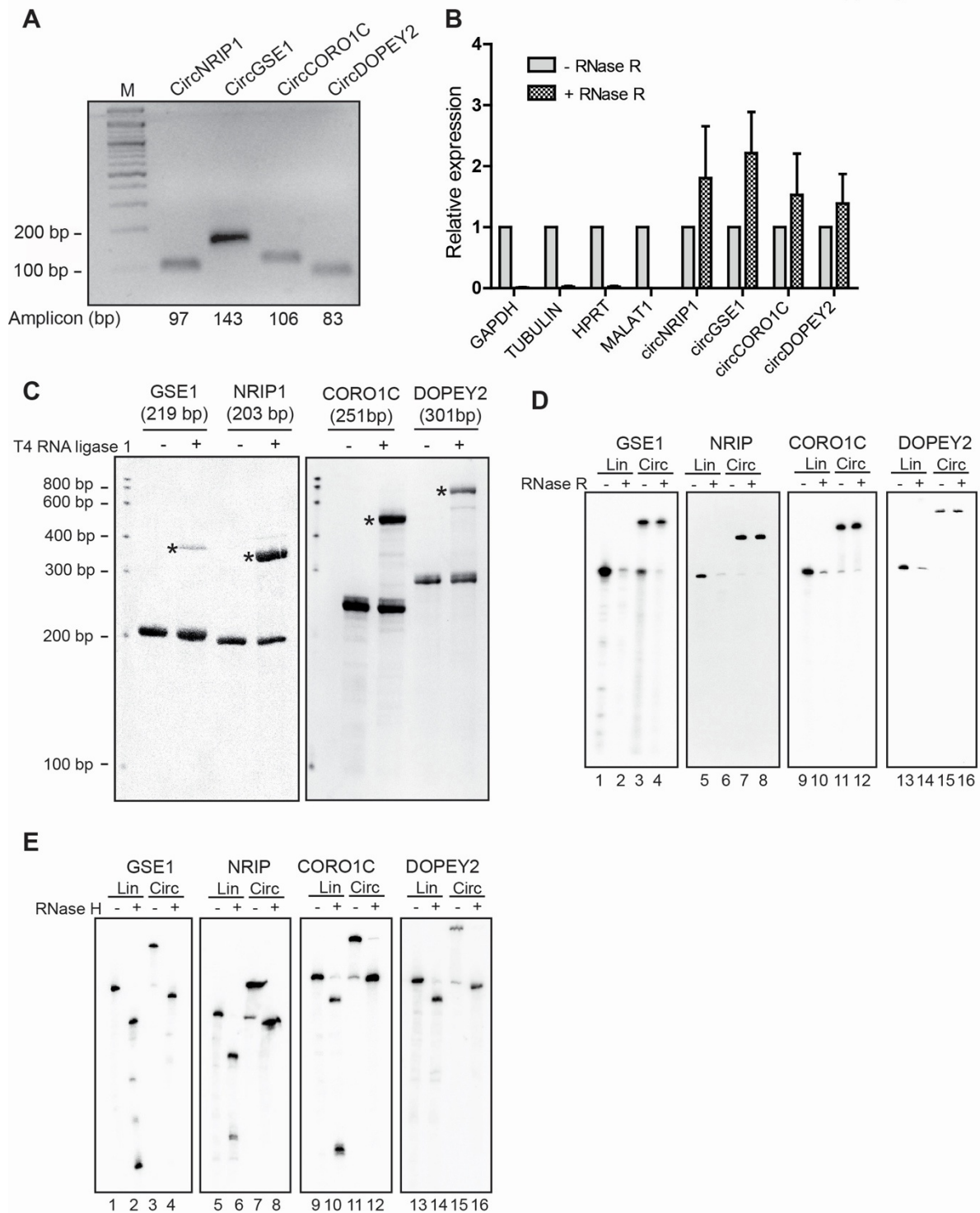


**Cell Reports, Volume 44**

**Supplemental information**

**Cytoplasmic DIS3 is an exosome-independent  
endoribonuclease with catalytic activity  
toward circular RNAs**

**Claudia Latini, Julian Eichlinger, Anna-Lisa Fuchs, Si-Nan Zhai, Hung Ho-Xuan, Gerhard Lehmann, Petar Glazar, Nikolaus Rajewsky, Astrid Bruckmann, Li Yang, Remco Sprangers, and Gunter Meister**

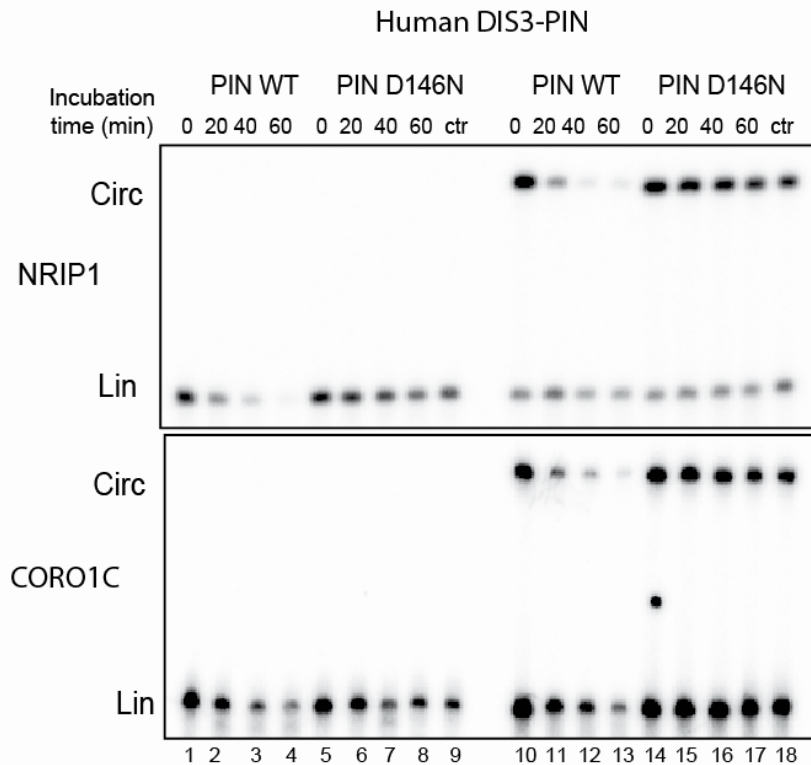


**Figure S1. *In vitro* synthesis and validation of natural circRNAs, Related to Figure 1**

(A) Agarose gel electrophoresis of RT-PCR products with divergent primers showing circularization of GSE1 NRIP, CORO1C and DOPEY2 in HEK 293 cells. The junction splice lengths are indicated. (B) Total RNA was extracted from HEK 293 cells and treated with RNase R. RT-PCR shows that the 4 circRNAs candidates are resistant to RNase R digestion differently from the negative controls GAPDH, MALAT1, TUBULIN and HRTPK. (C) PAGE analysis of

the *in vitro* circularization RNA products. The mobility of the putative circular RNAs is indicated with asterisks (\*); the circRNA lengths are also indicated. CircRNAs migrate lower compared to their linear counterparts in agarose gel. (D) Synthetic circular and linear RNAs were treated with RNase R and analysed by northern blotting against the indicated RNA. CircRNAs are resistant to RNase R digestion, while linear RNAs are degraded. (E) Synthetic linear and circular RNAs were treated with RNase H in the presence of a specific antisense DNA oligonucleotide and analyzed by northern blot. Northern blot analysis showing two RNA products for linear RNAs and only one linear fragment for circRNAs whose size correspond approximately to the linear counterpart.

**A**



**B**

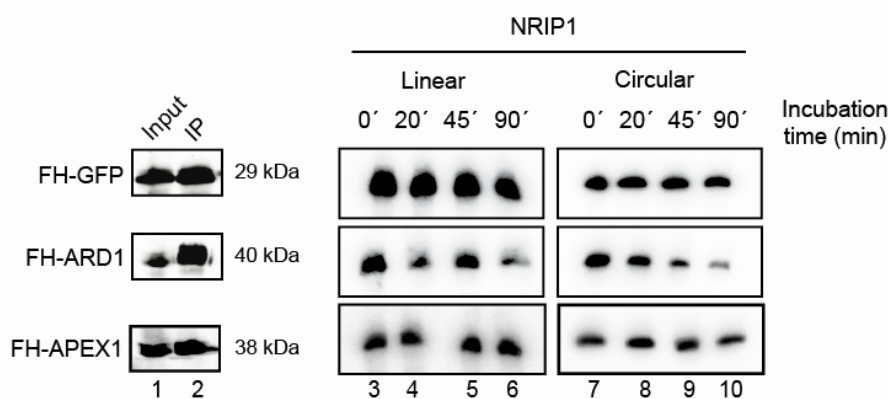


**Figure S2. RNA degradation assays with recombinant human DIS3 PIN domain versions and resin immobilized endonucleases, Related to Figure 2-4**

(A) Cleavage reactions using radiolabeled linear and circular NRIP and CORO1C together with the human recombinant DIS3 PIN domain proteins: Wild type DIS3 PIN (PIN WT) and mutant D146N DIS3 PIN (PIN D146N). (B) In the left panel, Flag-HA tagged endonucleases were immunoprecipitated with flag beads and detected by western blot using anti HA antibodies. In the right panel, Urea Gel-electrophoresis analyses represent the incubation of labelled linear and circular NRIP1 with resin-immobilized indicated proteins at different time points. FH-GFP served as negative control.

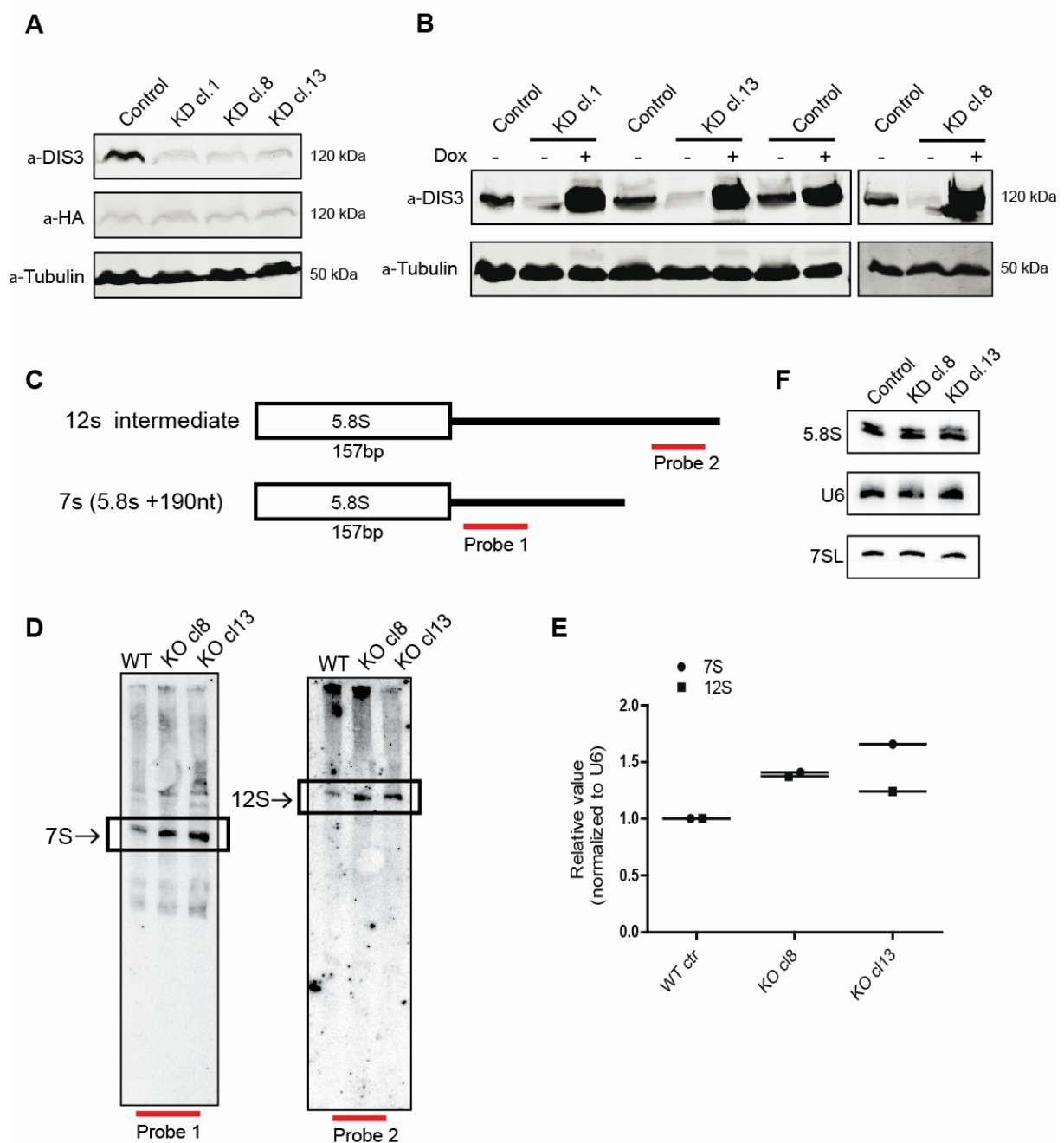


**Figure S3. Validation of DIS3 CRISPR/Cas9 knockdown cells, Related to Figure 3**

(A) Lysates from WT, and selected Dis3 knockout T-REx-293 cells (cl1, cl8, cl13) were analyzed by western blot against Dis3 and HA. b-tubulin served as loading control. A leaky expression of Dis3 is detected. (B) Western blot from WT and selected Dis3 KO T-REx-293 cells (cl1, cl8, cl13) after doxycycline treatment. Western blot shows that the expression of FH-Dis3 is rescued in all selected Dis3 KO clones (cl1, cl8, cl13). Dis3 proteins were detected using anti-DIS3, anti-HA antibodies. b-tubulin was used as loading control. (C) Schematic overview of the designed probes used for detecting 5.8S precursors and intermediates. Red bars represent the antisense DNA oligos used as northern blot probes. Probe 1 detects the shorter 3-extended 5.8S species, the 7S intermediate. Probes 2 was used to detect the longer 3-extended 5.8S, the 12S intermediate. (D) Total RNA was isolated from WT, and selected DIS3 knockout

T-REx-293 cells (cl1, cl8, cl13) and analyzed by northern Blot using the mentioned probes. The black frames underline the specific 5.8s precursors: 7S and 12S. (E) The 7S and 12S signal intensities were calculated followed U6 normalization and phosphor image analysis and are represented in the graph. (F) Northern blots from (D) were probed with 7SL, U6 and 5.8S to serve as a loading control.

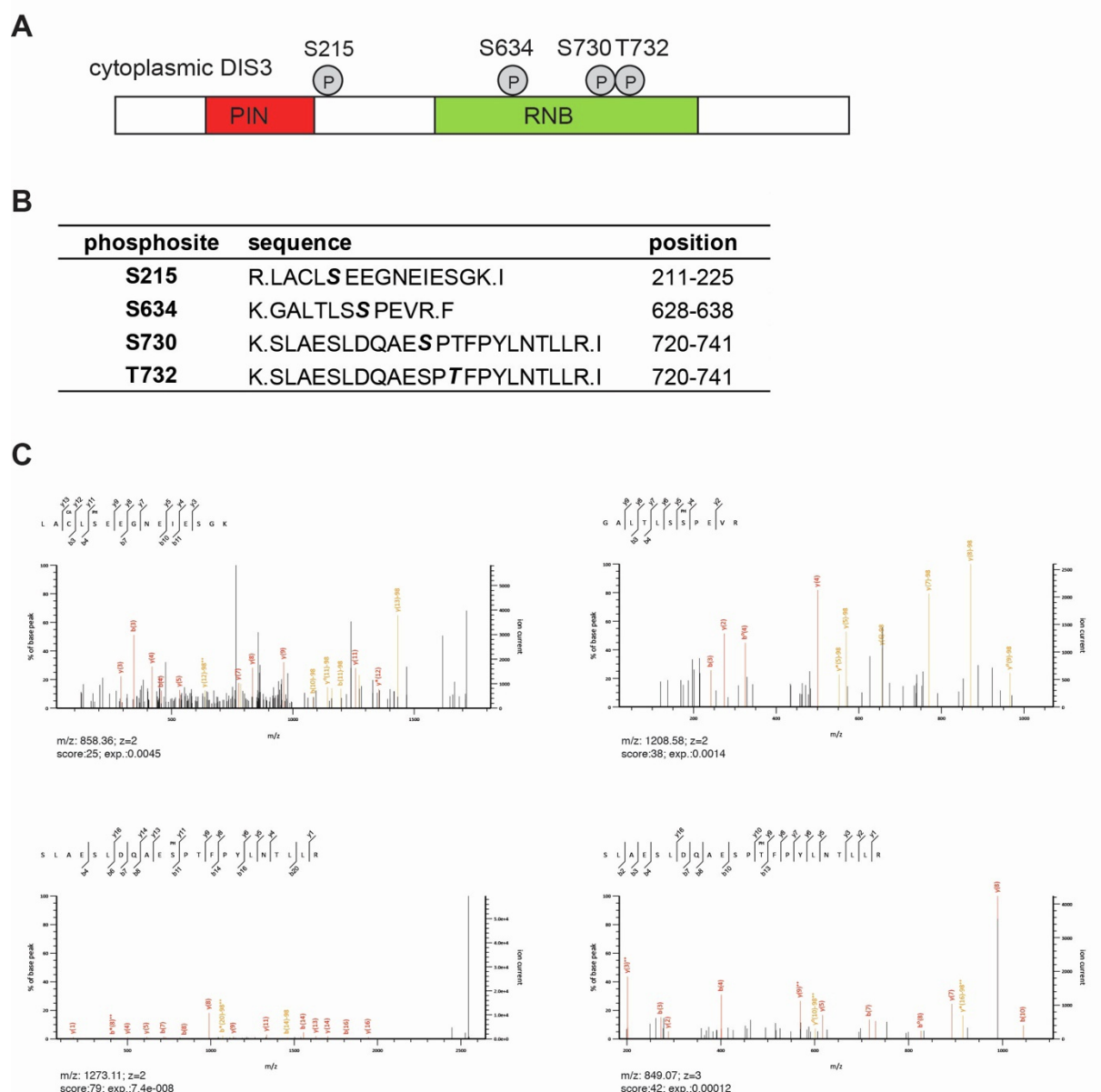


**Figure S4. Identification of human DIS3 phosphosites, Related to Discussion**

(A) Schematic representation of the DIS3 domain organization with the positions of phosphosites identified by mass spectrometry in cytoplasm. (B) Phosphorylated DIS3 peptides detected by mass spectrometry. (C) CID fragment spectra of phosphorylated human DIS3 peptides from a LC-UHR-QTOF run. The mass-to-charge ( $m/z$ ) ratios, the charge ion ( $z$ ), the Mascot ion score (score) and the expectation value (exp) of the peptides are reported.